Electronic Supplementary Information (ESI)

1. XRD and RBS analyses of a single Ta_2O_{5-x} switching layer

In X-ray diffraction (XRD) patterns of Ta_2O_{5-x} films deposited on SiO_2/Si substrates (Figure S1a), no obvious diffraction peaks were observed, demonstrating the formation of amorphous-phase Ta_2O_{5-x} films. Based on RBS spectra of the Ta_2O_{5-x} film (Figure S1b), the composition of the films used herein was determined to be $Ta_2O_{4.86}$.

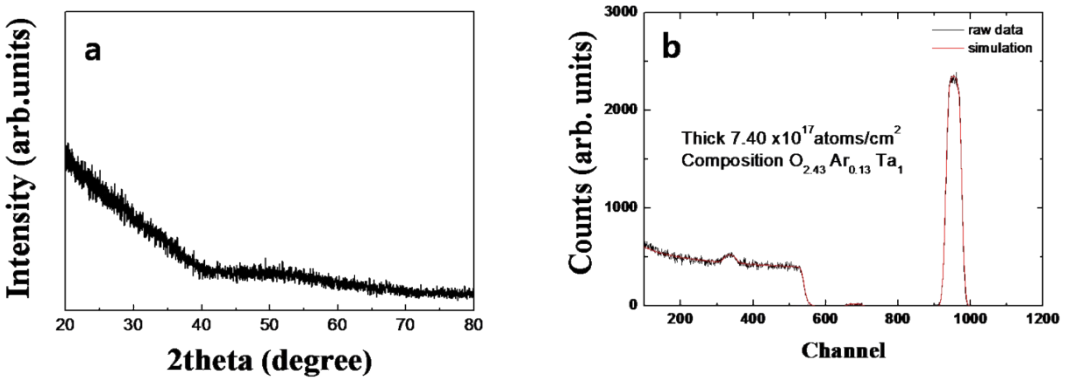

Figure S1. (a) XRD patterns of the Ta_2O_{5-x} layer. (b) RBS profiles of the Ta_2O_{5-x} layer.

2. TEM and AES analyses of a basic Pt / Ta_2O_{5-x} /Ta switching cell

In a cross-sectional TEM image of one unit switching element used for the basic Pt / Ta_2O_{5-x} /Ta switching cell, a uniformly grown 20-nm-thick amorphous Ta_2O_{5-x} active layer was clearly identified, with sharp interfaces between the active layer and two electrodes (Figure S2a). In Auger electron microscopy depth profiles of as-grown switching device (Figure 2Sb) revealed nearly constant oxygen concentrations at the Ta_2O_{5-x} layer region.

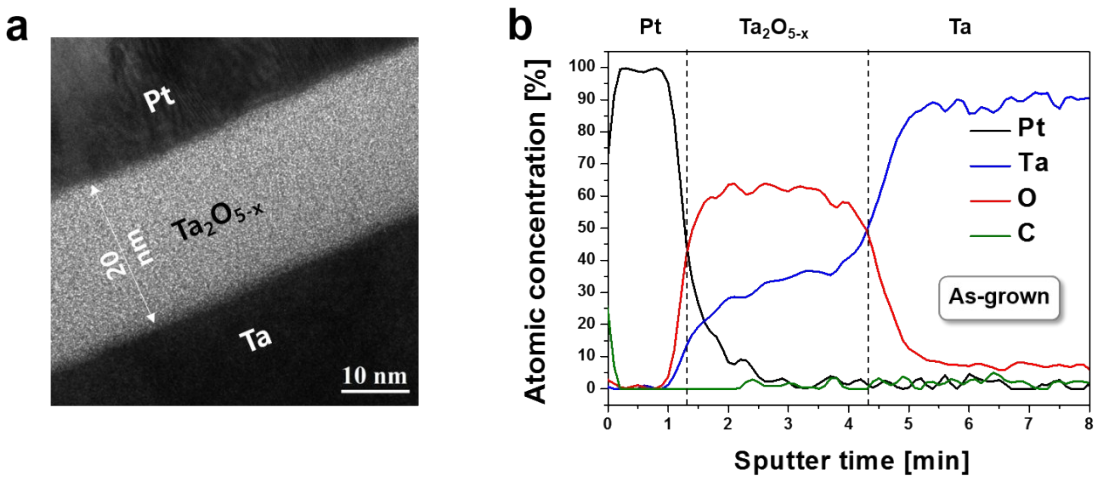

Figure S2. (a) TEM image of the Pt/Ta_2O_{5-x}/Ta switching cell. (b) AES depth profile results of the Pt/Ta_2O_{5-x}/Ta layer.

3. Various forming behaviors of the merged device depending on an initial resistance

Basically, there was a variation in the initial resistance among cells, as seen in Figure S3-1. However, it is not clear why each Pt/Ta_2O_{5-x}/Ta or Ta/Ta_2O_{5-x}/Pt device exhibited different initial resistances, depending on each cell. Typical initial resistance of each cell was about 10^5 Ω. One of the most striking findings was that the final RS behaviors were not associated with initial resistance and structural configurations, but strongly affected by the polarity of forming bias: That is, Type A or Type B RS behaviors were observed, depending on the forming bias polarity. Furthermore, it was found that the forming voltage (nearly ± 4 V) of Type B was larger than that (nearly ± 2 V) of Type A.

To further clarify the forming curve observed in Figure 1b, we have considered three different forming curves arising from the initial resistances of Types A and B. The first case indicated the forming curve described in the manuscript, in which Type A (SE1) has a higher initial resistance than that of Type B (SE2) as shown in Figure S3-2. The merged cell containing the above two switching elements provided the forming curve observed in Figure 1b under the whole forming process. As seen in this figure, the merged device displayed two forming steps at two different voltages of SE1 (red dashed line) and of SE2 (blue dashed line) upon the whole-forming process. In advance, the application of a negative forming bias to the merged device may mostly drop across the SE1 due to the high initial resistance and could allow the SE1 to switch to LRS at a lower voltage. After forming the SE1, most of the voltage drops across the SE2. Thus, the resistance of the merged device arises from the initial resistance of SE2 until reaching the forming of SE2. In addition, the resistance of the merged device was around 2.5 x 10^5 Ω in the range of -1.76 to -4.04 V. It may be interpreted as a superimposed behavior of two forming events of each SE1 and 2 SE2 during the whole forming process.

The second is the case when the SE1 and SE2 possess the similar initial resistances, as

shown in Figure S3-3. Since two switching elements have similar initial resistances, equal voltages drop on the SE1 and SE2 under a negative bias. Therefore, at first, the application of a negative forming bias to the merged device can allow the SE1 to switch to LRS at a lower voltage and then after forming the SE1, most of the voltage drops across the SE2. Thus, the resistance of the merged device arises from the initial resistance of SE2 until reaching the forming of SE2. As a result, the abrupt current jump arising from SE1 does not appear noticeably. And then the forming event of SE2 takes place with a continuously applied negative bias.

The third is the particular case, in which initial resistances of both switching elements are extremely high or Type B has a higher initial resistance than that of Type A. In this case, two forming steps does not appear as expected because of the above reason discussed, as shown in Figure S3-4. In addition, we also confirmed that an asymmetric I-V behavior takes places upon a whole-forming process, regardless of the initial resistance value.

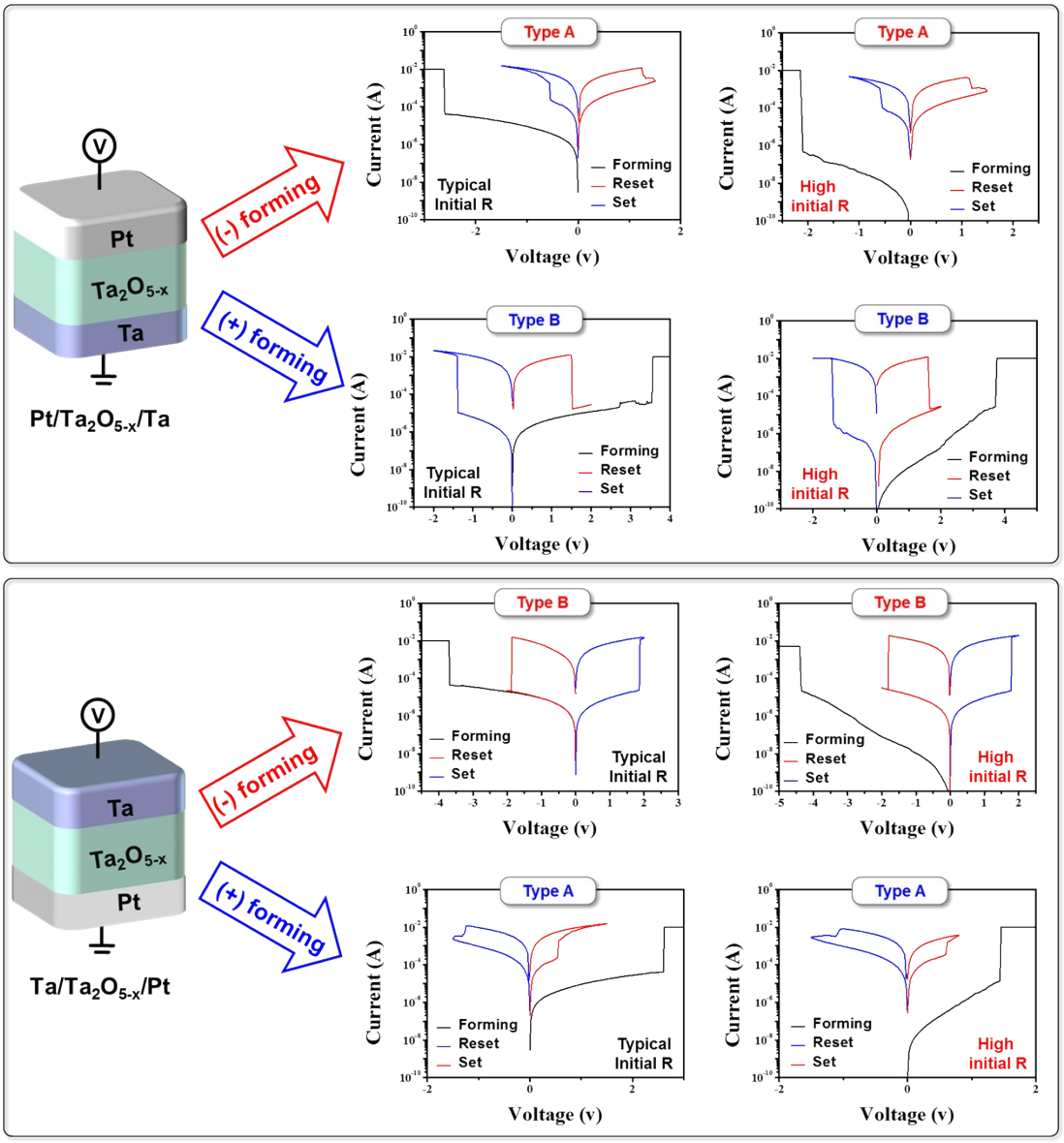

Figure S3-1. Various initial I-V curves of basic switching elements $Pt/Ta_2O_{5-x}/Ta$ and $Ta/Ta_2O_{5-x}/Pt$, reflecting various initial resistance values.

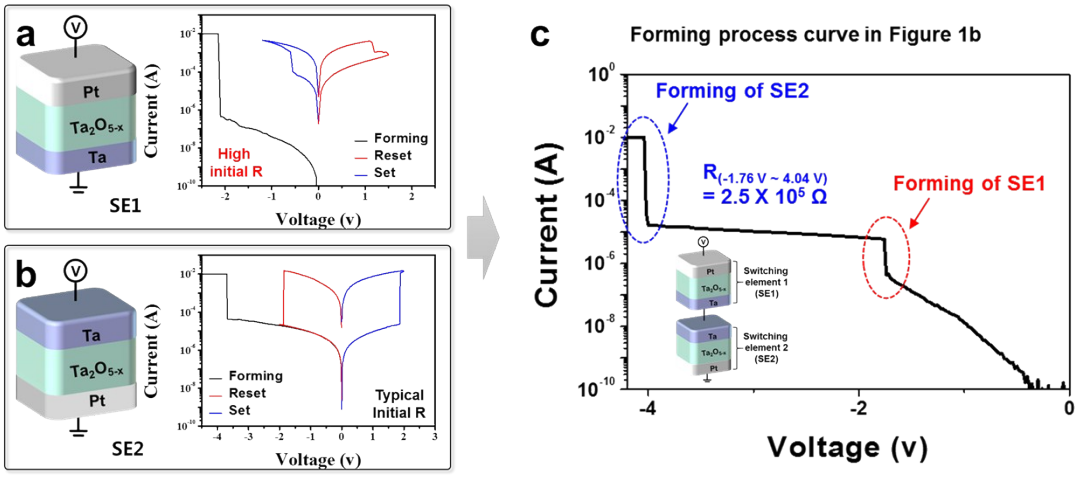

Figure S3-2. Initial I-V curves of (a) Pt/Ta_2O_{5-x}/Ta with a high initial resistance and (b) Ta/Ta_2O_{5-x}/Pt device with a typical resistance, respectively. (c) Re–plot of I-V curve highlighting the forming process curve of Figure 1b.

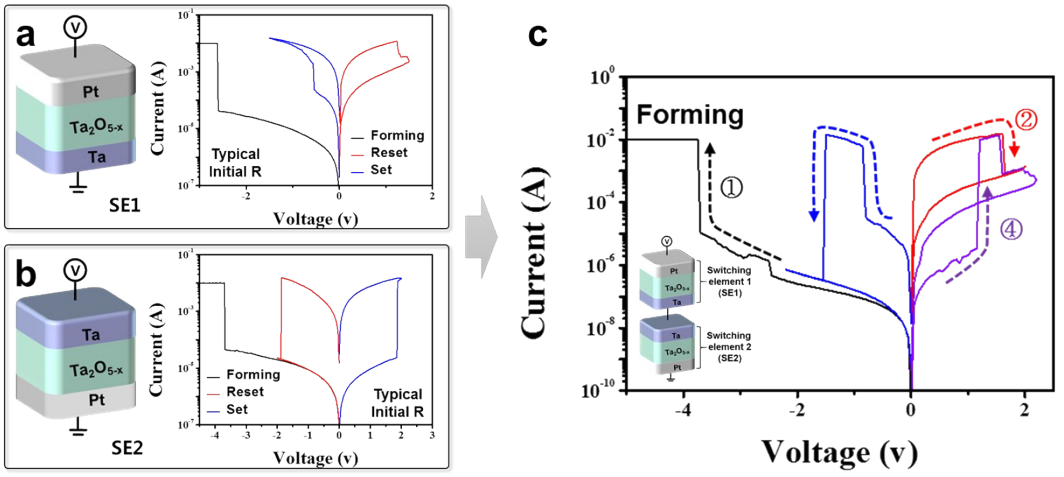

Figure S3-3. Example for the whole-forming process when both SE1 and SE2 possess the similar typical initial resistance (about 10^5 Ω).

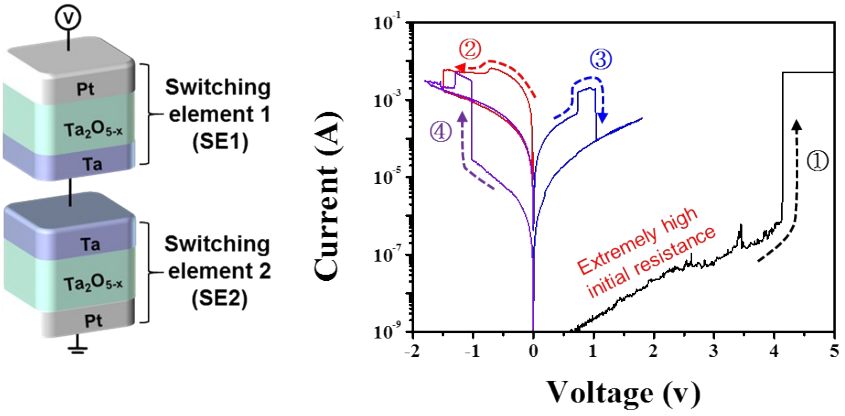

Figure S3-4. Asymmetric CRS features of the merged device via a whole-forming process, in which initial resistances of both switching elements are extremely high or Type B has a higher initial resistance than that of Type A

4. Asymmetric RS behavior of a completely stacked Pt/Ta_2O_{5-x}/Ta/Ta_2O_{5-x}/Pt device

We have examined resistive switching features of a completely stacked Pt/Ta_2O_{5-x}/Ta/Ta_2O_{5-x}/Pt frame device. Figure S4a exhibits the representative schematic of Pt/Ta_2O_{5-x}/Ta/Ta_2O_{5-x}/Pt CRS cell that are anti-serially connected from two bipolar Pt/Ta_2O_{5-x}/Ta switching elements without the use of electrical wire connection, where a Ta layer is commonly used as a middle electrode of CRS cell. As shown in Figure S4b, the completely stacked Pt/Ta_2O_{5-x}/Ta/Ta_2O_{5-x}/Pt frame device also confirmed the asymmetric CRS-like RS behaviors which were similar to the findings of the electrically merged device of Figure 1d.

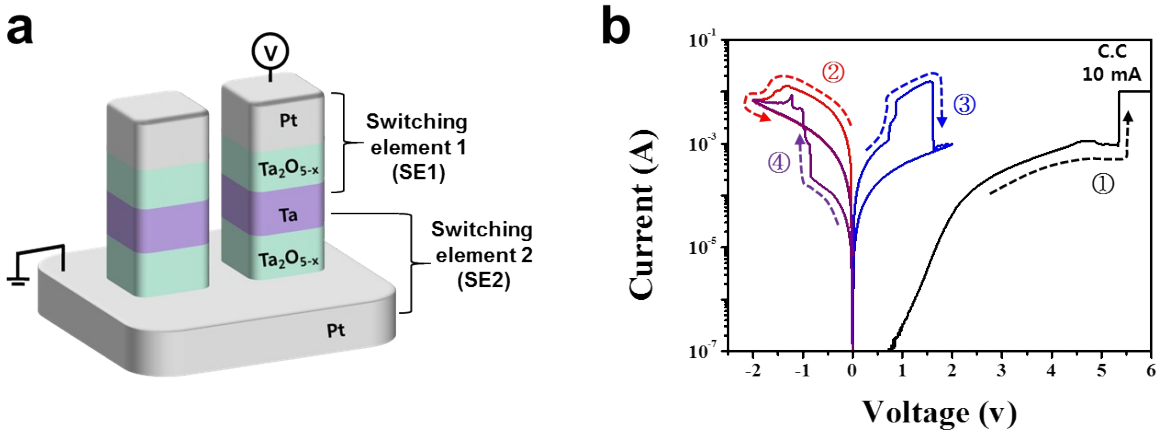

Figure S4. (a) Schematic and (b) asymmetric I-V features of the completely stacked Pt/Ta_2O_{5-x}/Ta/Ta_2O_{5-x}/Pt device consisting of two types of switching elements.

5. Various CRS-like features of a negatively formed merged device, depending on set/reset voltages of unit switching elements

Basically, typical CRS devices should show set/reset sequences under both positive and negative polarity sweep regions, as depicted in Figure S5a. However, under certain measurement and sample conditions, the CRS device provided several different I-V features in our work. As shown in the positive region of Figure S5b, a spike shape signal was obtained when the V_{set} of SE2 was comparable to V_{reset} of SE1. In addition, only a set transition (Figure S5c) was revealed when the V_{set} of SE2 was larger than V_{reset} of SE1, in which no reset event was observed. Therefore, these observations were likely due to the characteristics of unit switching elements. Furthermore, a voltage sweep interval was 0.05 V in our measurement. Thus, if the set/reset sequences arise within 0.05 V, the reset transition is not able to be observed due to the measurement limitation. Thus, we expect that since an individual unit switching element can have essential set/reset voltage distribution characteristics, the merged CRS device can also reveal various set/reset sequence behaviors depending on the characteristics of unit switching elements, together with the measurement limitation used in our work.

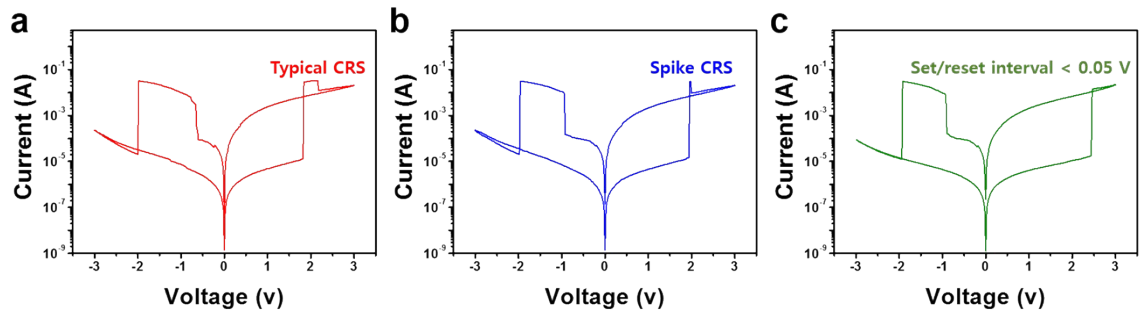

Figure S5. Various CRS-like behaviors of a negatively formed merged device, depending on

set/reset voltage contribution of unit switching elements and measurement limitation. (a) $V_{set} < V_{reset}$, (b) $V_{set} \sim V_{reset}$, and (c) $V_{reset} - V_{set} < 0.05$ V.

6. Continuously repeated measurement contributions to I-V responses of Types A and B

Typical I-V measurements of Type A and Type B devices during 100 continuous cycles indicate that the HRS of Type A (Figure S6a) is more stable than that of Type B (Figure S6b). In addition, Type B shows a wide variation in set and reset voltages. The resistive switching instability of Type B is attributed to the instability of the rupture and creation of filament paths, arising from the role of Joule heating in filament rupture. Figure S6c shows the extracted current values of the LRSs and HRSs obtained at 0.2 V, demonstrating the expected wider variation in the HRS current distribution of Type B.

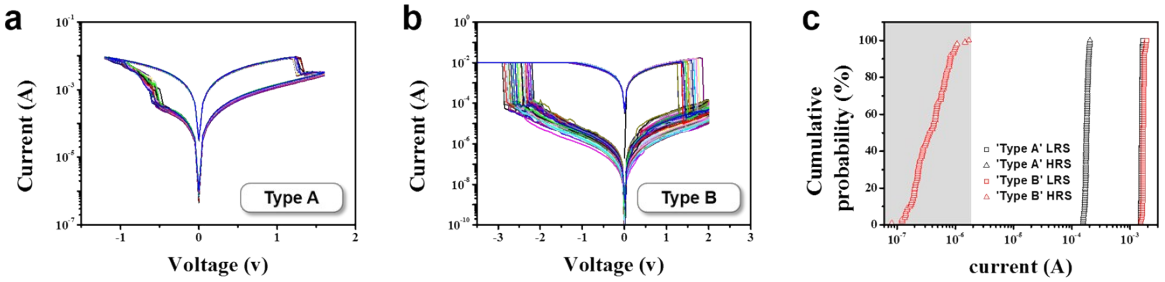

Figure S6. Typical I-V profiles of (a) Type A and (b) Type B devices, measured during 100 continuous cycles; (c) Cumulative distributions of LRS and HRS currents for both switching types.

7. Output features of a positively electroformed Pt/Ta_2O_{5-x}/Ta-Ta/Ta_2O_{5-x}/Pt device

To further verify the influence of bias polarity on the resulting RS properties, a positively electroformed Pt/Ta_2O_{5-x}/Ta-Ta/Ta_2O_{5-x}/Pt merged device was employed in addition to the negatively electroformed device discussed in the main text. As expected, clear triple-state RS features appeared, along with completely symmetric I-V curves. This confirmed that applying a voltage bias to the whole merged device during the forming steps affects the RS behaviors of each switching element. That is, the RS characteristics of a merged cell subjected to whole-device positive electroforming arise from the Type B properties of SE 1 combined with the Type A properties of SE 2, due to the electroforming-polarity-dependent I-V features of each type.

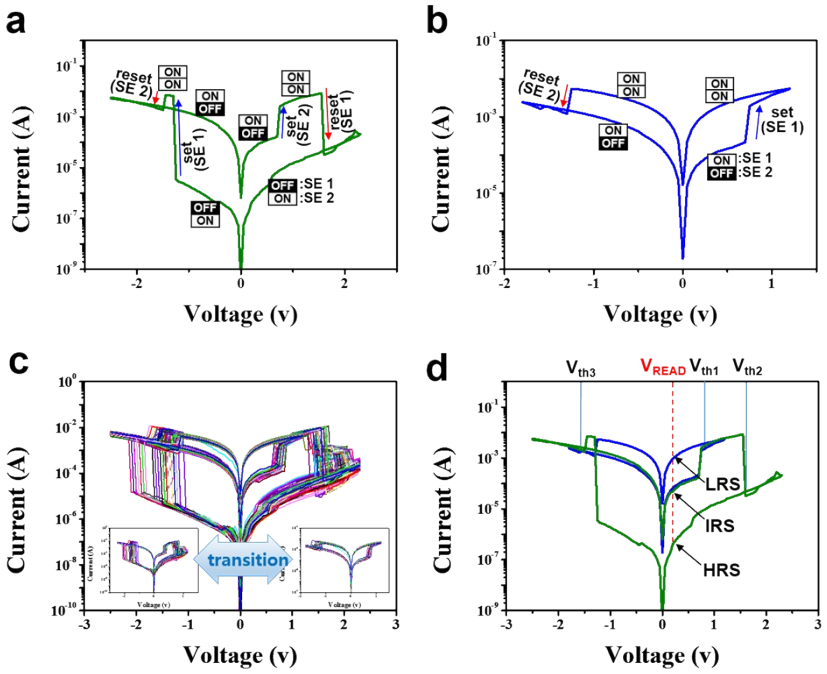

Figure S7. Triple-level RS plots of a positively electroformed Pt/Ta_2O_{5-x}/Ta-Ta/Ta_2O_{5-x}/Pt merged device. (a–b) Typical I-V characteristics of the merged device (a) measured in the range from -2.5 to +2.3 V and (b) taken in the range from -1.8 to +1.2 V; element states during various

stages of the voltage sweep are labeled using ON and OFF symbols. (c) Bias-dependent transition between the asymmetric CRS-like and bipolar RS behaviors; (c, insets) typical I-V characteristics of each switching element measured over 100 cycles. (d) Demonstration of triple-level states of LRS, IRS, and HRS; threshold and read voltages are indicated.

8. Identification of asymmetric IRS behavior.

Low temperature measurements in the range of 50 K-300 K were carried out to clarify the conduction of IRS_{CRS}. As shown in the Figure S8a, the resistance of IRS decreased with increasing temperatures, reflecting the semiconductor-like behavior arising from the summed effect of LRS of Type B (metallic-like conduction) and HRS of Type A. Thus, the asymmetrical behavior may originate from Type A RS behavior. According to the above temperature-dependent observations of the IRS_{CRS} resistance, it is acceptable that the Pt/semiconductor-like Ta_2O_{5-x} interface can form Schottky contacts due to the work function difference between Pt and TaO_x materials in HRS, while the Ta_2O_{5-x}/Ta interface creates the ohmic contact behavior owing the low work function of Ta electrode, as seen in the Figure S8b of the band diagram. Thus, the rectifying behavior can occur in the HRS of Type A RS when the reverse and forward directions are in a negative and positive regions, respectively. Then, the asymmetric behavior appears in a negatively electroformed IRS_{CRS} corresponding to the OFF state of SE 1 of the merged device, as seen in the Figure 4a.

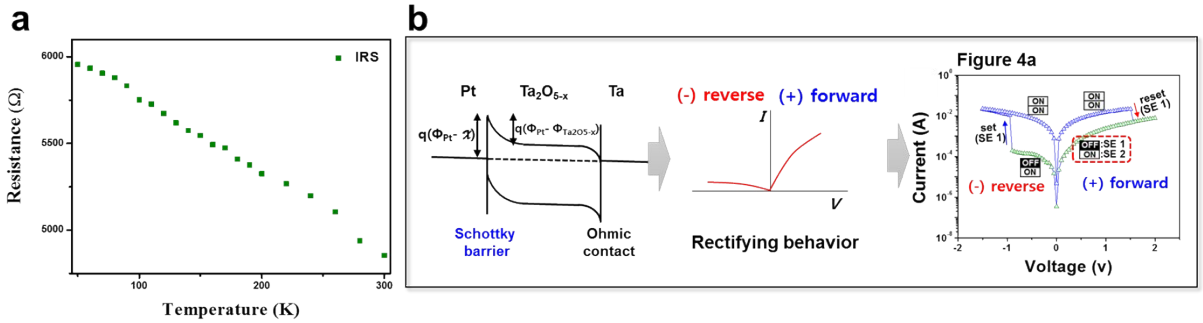

Figure S8. (a) Temperature-dependent IRS_{CRS} resistance showing a semiconductor-like behavior. (b) Possible schematics for the nature of asymmetric IRS_{CRS} behavior arising from contact issue in Type A of SE 1 of the negatively electroformed merged device.

9. Performance of the merged device under a pulse operation

We have also examined the performance of the merged device under a pulse mode operation by using the Keithley 4200 including a pulse-measure unit (PMU). Figure S9a shows a schematic voltage pulse diagram used for this test, where 100 and 50 μsec pulse widths are selected for HRS, IRS, LRS write pulse and 10 μsec pulse width is chosen for identifying the cell states. The write pulse amplitudes for HRS, IRS, and LRS were -4, +4,-2 V that are higher than those determined by the typical dc voltage sweep operation, respectively. As shown in the Figure S9b, the tri-states arising from a symmetric RS behavior were clearly identified under the program pulses with a width of 100 and 50 μsec in the negatively formed merged device.

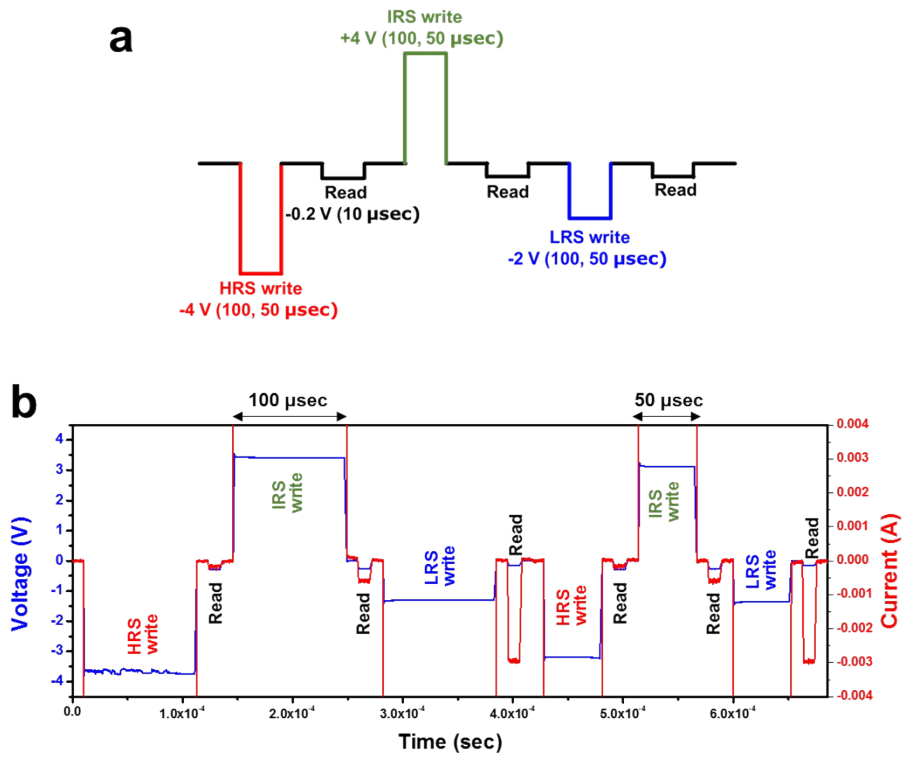

Figure S9. (a) Schematic illustration of the voltage pulse for a pulse mode operation. (b) Pulse properties of the merged device. This measurement shows the tri-state RS behavior of the negatively formed merged device. Each negative read pulse (-0.2 V) is followed by a write pulse with positive or negative polarity respectively.

10. Pt electrode dependence of resistive switching behavior: tests on a Pt/Ta_2O_{5-x}/Pt matrix

To gain further insight into the Type B reset process, a Pt/Ta_2O_{5-x}/Pt cell was tested; that is to say, an element was tested that replaced the bottom Ta electrode with a bottom Pt electrode (Figure S10a). This device exhibited a sharp current drop during its reset process (Figure S10b), representing the rupture of filament paths due to local thermal heating (Figure S10c). This finding provides indirect evidence that the Ta bottom electrode plays a crucial role in the Type B reset process.

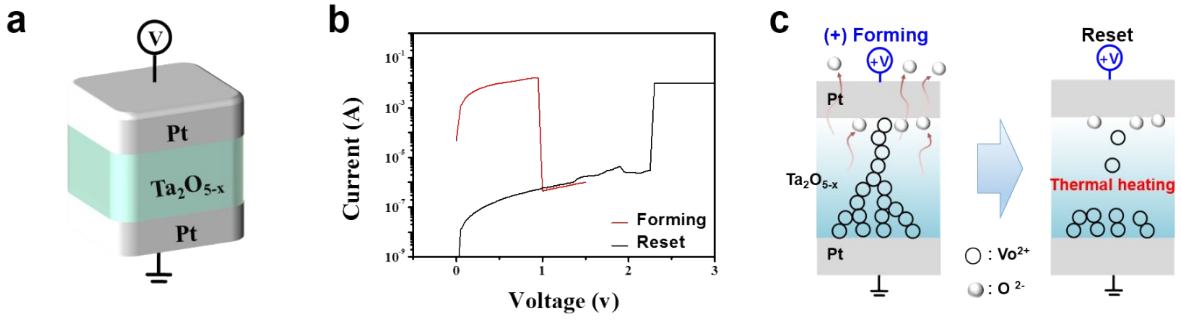

Figure S10. (a) Schematic of a Pt/Ta_2O_{5-x}/Pt switching element with a Pt bottom electrode. (b) I-V features showing unipolar switching behavior. (c) Possible mechanism to explain the unipolar switching characteristic, including the rupture and creation of conducting filaments induced by bias-polarity-dependent Joule heating effects; open and filled circles correspond to oxygen vacancies and oxygen ions, respectively.